OPEN ACCESS

University of Dundee

University of Dundee

Physical properties and functional alignment of soft-embalmed Thiel human cadaver when used as a simulator for ultrasound-guided regional anaesthesia

Munirama, S.; Eisma, R.; Columb, M.; Corner, G. A.; McLeod, G. A.

Published in:
British Journal of Anaesthesia

DOI:
10.1093/bja/aev548

Publication date:
2016

Document Version
Peer reviewed version

Link to publication in Discovery Research Portal

Citation for published version (APA):
Munirama, S., Eisma, R., Columb, M., Corner, G. A., & McLeod, G. A. (2016). Physical properties and functional alignment of soft-embalmed Thiel human cadaver when used as a simulator for ultrasound-guided regional anaesthesia. *British Journal of Anaesthesia*, *116*(5), 699-707. https://doi.org/10.1093/bja/aev548

General rights
Copyright and moral rights for the publications made accessible in Discovery Research Portal are retained by the authors and/or other copyright owners and it is a condition of accessing publications that users recognise and abide by the legal requirements associated with these rights.

• Users may download and print one copy of any publication from Discovery Research Portal for the purpose of private study or research.
• You may not further distribute the material or use it for any profit-making activity or commercial gain.
• You may freely distribute the URL identifying the publication in the public portal.

Take down policy
If you believe that this document breaches copyright please contact us providing details, and we will remove access to the work immediately and investigate your claim.

Download date: 04. May. 2023

The Physical Properties and Functional Alignment of Soft Embalmed Thiel Human Cadaver when used as a Simulator for Ultrasound Guided Regional Anaesthesia.

Dr Shilpa Munirama
Consultant Anaesthetist
Manchester Royal Infirmary
shilpa.m@hotmail.co.uk

Dr Roos Eisma
Centre for Anatomy and Human Identification,
University of Dundee
r.eisma@dundee.ac.uk

Malachy Columb
Intensive care Unit
Wythenshawe Hospital,
South Manchester University Hospitals,
Manchester, UK
mlacolumb@doctors.org.uk

Prof George A Corner
Head of Instrumentation, Department of Medical Physics
Ninewells Hospital & Medical School
g.a.corner@dundee.ac.uk

Dr Graeme A McLeod
Consultant & Honorary Clinical Professor
Institute of Academic Anaesthesia
Ninewells Hospital & Medical School
g.a.mcleod@dundee.ac.uk

Corresponding Author
Current address
Graeme A McLeod
Consultant Anaesthetist & Honorary Clinical Professor
Institute of Academic Anaesthesia
Ninewells Hospital & Medical School
g.a.mcleod@dundee.ac.uk

Keywords

Cadaver

Regional anaesthesia

Ultrasonography

Elastography

Background. We evaluated the physical properties and functional alignment of the soft embalmed Thiel cadaver by assessing tissue visibility; measuring its acoustic, mechanical and elastic properties; evaluating its durability in response to repeated injection; and aligning images with humans.

Methods. In 4 soft embalmed Thiel cadavers we conducted 3 independent studies. We assessed: (1) soft tissue visibility in a single cadaver for 28 weeks after embalming; (2) the displacement of tissues in response to 1ml and 5ml interscalene and femoral nerve blocks in a single cadaver; and (3) the stiffness of nerves and perineural tissue in two cadavers. We aligned our findings with ultrasound images from 3 patients and 1 volunteer. Durability was qualified by assessing B-Mode images from repetitive injections during supervised training.

Results. There was no difference in visibility of nerves between 2 and 28 weeks after embalming, [geometric mean ratio 1.13(95%CI: 0.75 - 1.68), P=1.0]. Mean tissue displacement was similar for cadaver femoral and interscalene blocks [geometric mean ratio 1.02(95%CI: 0.59 - 1.78), P=0.86]; and 1ml and 5ml injection volumes [geometric mean ratio 0.84(95%CI: 0.70 - 1.01), P=0.19]. Cadavers had higher intraneural than extraneural stiffness (Young's modulus) [geometric mean ratio 3.05(95%CI: 2.98 - 3.12), P < 0.001]; and minimal distortion of anatomy when conducting 934 left sided interscalene blocks on the same cadaver over 10 days.

Conclusions. The soft embalmed Thiel cadaver is a highly durable simulator that has excellent physical and functional properties that allow repeated injection for intensive ultrasound guided regional anaesthesia training.

Introduction

The drive to improve safety and quality in healthcare, allied to limitations in anaesthesia training time has encouraged the development of simulation outside the operating room[1]. Ultrasound guided regional anaesthesia (UGRA) simulators include plastic phantoms[2], tofu, animal tissue, fresh frozen cadavers[3] and virtual reality models[4]. All have an educational role because the structural fidelity of a simulator does not necessarily result in the successful transfer of knowledge and skills to the work place.[5] Successful simulator based learning is achieved by aligning functional tasks within an appropriate context whereby educational needs and pre-existing skills are matched to task difficulty and simulator complexity[6].

A new development in medical simulation is the soft embalmed Thiel human cadaver[7]. Cadavers are life-like, have full movement of joints, and may be used for 3 years.[8, 9] Skin and tissue are soft and moist, providing good conditions for ultrasound, and fascial integrity is retained, giving feedback during needle insertion[10, 11]. The physical characteristics of the cadaver may be attributed to Thiel's embalming mixture consisting of monopropylene glycol, ammonium nitrate, potassium nitrate, sodium sulphite, boric acid, chlorocresol, and a small amount of formaldehyde. This combination has anti-infective properties. On arrival in the mortuary embalming fluid is infused through an artery (femoral or brachial) and a vein (superior sagittal sinus or brachial vein). Cadavers bodies are submerged in an tank of embalming fluid for 4 to 6 months. Thereafter bodies are removed and kept in sealed plastic bags without need for refrigeration.

We are currently measuring trainee UGRA competence using expert supervised one-to-one training using the soft embalmed Thiel cadaver. In doing so, we considered it important to measure the physical properties and functional alignment[6] of the soft embalmed Thiel cadaver: that it looked like, felt like and responded to perineural injection in a similar way to that experienced clinically, and that it was robust enough to tolerate frequent block repetition

over several days. Our intention was not to compare measurements with matched humans, but rather demonstrate that the soft embalmed Thiel cadaver is a simulator that provides conditions with the potential to support intensive training by suspending belief.

Therefore, the primary objective of our pilot study was to determine the physical and functional alignment of the soft embalmed Thiel human cadaver by evaluating the visibility of tissues after 28 weeks embalming; measuring the cadavers' acoustic, mechanical and elastic properties; assessing the durability of tissues in response to repeated injection; and aligning our findings with typical ultrasound images from humans. Images in humans were not quantitatively analysed.

Methods

Three independent cadaver studies, approved by the Thiel Cadaver Ethics Advisory Committee at the University of Dundee, UK, were undertaken in the Centre for Anatomy and Human Development (CAHID) and overseen by the Anatomy Scientific Officer according to the Anatomy Act (Scotland) 2006.

Written, informed consent was gained from three patients and one volunteer to provide comparator images and videos representative of standard clinical practice; our surgical consent form includes a section for such patient approval. Patient anonymity was ensured using Caldicott Guardian approval, NHS Tayside, Data Protection Reg. No. Z8537226. The East of Scotland Medical Ethics Committee stated in writing that full ethical committee approval was not required as comparative clinical data was obtained from examples of routine clinical practice in which patients received standard UGRA using B-Mode ultrasound by the anaesthetist routinely managing the operating list. All elastography images were obtained on a secondary screen, but were not used to guide UGRA management as no operator had been trained to use or interpret elastography images.

Tissue Visibility

We scanned the left interscalene, axillary, femoral and popliteal regions of a single soft embalmed Thiel cadaver 2, 3, 5, 8, 11, 14 and 28 weeks after death. For scanning, we used a 5 to 10 MHz linear B-Mode ultrasound probe (Zonare, Palo Alto, CA) or, in the case of the sciatic nerve, a 3 to 9 MHz curvilinear ultrasound probe. Images were assessed by two independent raters blinded to the site and timing of scans. Both raters assessed the visibility of the C6 nerve root, the axillary radial, femoral and sciatic nerve in the popliteal fossa using a seven point ordinal scale between 1 (extremely poor visibility) and 7 (extremely good visibility). Each rater, using the same scale, noted the visibility of the corresponding muscles – anterior scalene, coracobrabrachialis, iliacus and biceps femoris - and corresponding arteries - carotid, axillary, femoral and popliteal.

Tissue displacement and brightness

In a second soft embalmed Thiel cadaver, we evaluated the mechanical and acoustic response to repeated injections and 1ml and 5ml volumes of injectate by measuring the area of displacement and brightness respectively of tissues during 16 interscalene and 16 femoral nerve blocks. We chose these block sites because our experience was that patterns of spread secondary to local anaesthetic injection are distinct for each block. We randomised our injections to equal numbers of 1ml and 5ml injections using a computer generated sequence of numbers. We block randomised to 1ml volume on our first study day, then repeated blocks using 5ml on the following day in order to assess any damage to the cadaver, and evaluate any accumulation of perineural fluid. A single experienced anaesthetist performed blocks using a 5 to 10 MHz linear B-Mode ultrasound probe (Zonare, Palo Alto, CA). After identifying the nerve of interest, we inserted a 50mm bevelled regional block needle (Braun, Sheffield, UK) in-plane to the ultrasound probe and injected Thiel

embalming solution. We recorded ultrasound images on a split display with the B-Mode image on the right and strain elastogram image on the left of the screen. Blocks were repeated every 5 to 10 minutes. The operator was not blinded to the elastogram image, as it is not possible to guide needle tip position or identify nerve location using this colour modality. We uploaded videos to Santesoft DICOM reader, converted each to TIFF files and uploaded them to ImageJ (v1.47, NIH, Washington DC).

Strain indicates relative displacement and is a unit-less entity. Therefore we measured the area of the coloured strain pattern, representing tissue displacement, on the elastogram during injection. Colour elastograms were converted to grayscale images, scaled in pixels cm^{-1}, then further transformed to a binary image[12]. The area of tissue displacement was visualised in black and demarcated from a white background on every 5^{th} image using a yellow tracing tool. ImageJ software also measured the brightness of area of displacement within the grayscale image using an ordinal 256 point scale between 0 (black) and 255 (white).

We also collected elastography images from videos of two patients. One received an interscalene block and the other a femoral nerve block. Blocks were conducted using the same technique as described using 1ml and 5ml perineural injections of 0.2% ropivacaine for interscalene block and 0.15% ropivacaine for femoral block.

Stiffness

We quantified the stiffness of the soft embalmed Thiel cadaver by measuring Young's elastic modulus over and adjacent to the interscalene nerve roots, median nerve and sciatic nerve in the popliteal fossa using shear wave elastography (SWE). SWE has shown good inter-observer and test-retest reproducibility measuring muscle stiffness in volunteers[13]. With

SWE, ultrasonic waves focused into a cone generate shear waves at multiple levels that are detected at rates up to 20,000Hz, 200 times faster than standard ultrasound. Young's elastic modulus is calculated according to the following equation $\mathrm{E} \simeq 3.\rho.c^2$ where: E = Young's elastic modulus; ρ = the density of tissues; c = the speed of sound through tissue; and 3 = a recognised approximation between shear modulus and Young's modulus[14]. The higher Young's Modulus, the higher tissue stiffness and vice versa.

We imaged the interscalene region because we have recently demonstrated the interscalene nerve roots in colour in a single volunteer using SWE and identified a threefold difference between intraneural and extraneural Young's modulus[15]. Moreover, our unreported previous work, scanning 11 colleagues between the ages of 25 and 50 years in the laboratory, showed that mean (SD) Young's modulus within the C6 nerve root was 22.8 (6.7) kPa and in perineural tissue 7.4 (2.6)kPa. We chose to assess the median nerve for two reasons: first, B-Mode scanning of the median nerve at the mid-forearm shows the characteristic subepineural mixed echogenic pattern of fascicles and interstitial tissue; and second, the stiffness of upper limb muscles in flexion and extension has been recently defined[16] using SWE in a large number of male and female volunteers, over a 70 year age span. We measured the stiffness of the popliteal sciatic nerve because the ratio of neural to non-neural tissue is less than within the interscalene nerve root[17] and we wished to determine if this was reflected in changes in nerve stiffness.

Two anaesthetists trained in SWE identified the interscalene nerve roots, median and sciatic nerves in two independent soft embalmed Thiel cadavers using B-Mode ultrasound. Once a satisfactory grayscale image was obtained using a 2 to 5MHz curvilinear probe (Supersonic Imagine, Aix-en-Provence), SWE superimposed a colour map of Young's elastic modulus onto an adjacent, identical B-Mode image, which was used for analysis. Each rater independently

selected a circular region of interest (ROI) 3 mm in diameter corresponding to the centroid of each nerve or nerve root and to an area just outside but not touching the epineurium consisting of a mix of connective tissue and adjacent muscles. The extraneural placement of the ROI was standardised and overlapped either anterior salene, flexor digitorum superficialis or biceps femoris outside the paraneural sheath of the sciatic nerve. Each intraneural and extraneural measurement was repeated 20 times. No injections were performed. The primary end point was the geometric mean (95%CI:) Young's modulus (kPa) of paired intraneural and extraneural ROIs at interscalene, median and sciatic nerve sites. Secondary objectives were to determine the effect of neural pairs, cadaver, site, and operator on Young's modulus. Computer generated block randomisation was undertaken to nerve location with equal allocation to cadaver, location and operator. Operators were not blinded to location or block because a high level of knowledge and skill was required to perform the scan. We also scanned the interscalene groove of a patient and the forearm median nerve and popliteal sciatic nerve of a 56 year old volunteer using SWE ultrasound. We scanned a volunteer because we rarely conduct mid-forearm blocks. We chose the median nerve in the forearam because ultrasound images of this nerve often usefully highlight the characteristic mixed echogenicity pattern of fascicles and connective tissue

Durability

We evaluated the durability of the soft embalmed Thiel cadaver in a separate study testing the feasibility of eye-tracking technology as a tool to quantify the competence and learning curves of anaesthetic trainees. Interscalene blocks were repeatedly performed on the left side of the neck on the same cadaver over a 10-day period. This study was approved by the University of Dundee non-clinical Ethics Committee. When the tip of the block needle (Sonoplex, Pajunk, Newcastle) was positioned between the C5 and C6 nerve roots, a test dose between 0.5ml and 1ml was administered. Each trainee performed a maximum of 60

blocks over 3 hours. In order to assess the durability of Thiel tissue, B-Mode images were recorded on day 7 at 0900h before session 13 and at 1500h after session 14, and then repeated on day 10 at the same times for sessions 19 and 20.

Statistical and Power Analysis

All data distributions were assessed using probability plots. In order to take account of the dependency of repeated continuous measurements, we used a repeated measures linear mixed effects regression model and tested for covariates and their interactions. Data was log transformed for analysis, then anti-logged and presented as the geometric mean. Differences between means are given as the geometric mean ratio (95%CI:). Significance was defined at $P<0.05$ (two-tailed). Analyses were performed using Number Cruncher Statistical Systems (NCSS) 2007, NCSS Inc., Kaysville UT, RStudio 0.98.978 – © 2009-2013 and GraphPad Prism 6, La Jolla, CA. We converted images using Adobe Photoshop CC 2015.0.0., San Jose, CA.

In order to power our strain elastography study, we calculated that using two blocks (interscalene, femoral) and two volumes (1ml and 5ml) and assuming $\alpha = 0.05$, $\beta = 0.80$, effect size = 0.6, and using ANOVA (G3Power, University of Dusseldorf) we needed 32 injections to show a difference between blocks.

In order to power our nerve and tissue stiffness study, we used data from a pilot Thiel cadaver study whereby the geometric mean (95% CI:) intraneural Young's modulus was 44.2 kPa and extraneural Young's modulus 12.8 kPa. Powering the study at 90%, to find as significant at $P<0.05$ a doubling of log transformed elastic modulus we required a minimum

of N=17 paired measures per combination of anaesthetist and site. Therefore, a total of 240 images were taken (2 cadavers, 3 nerves, 2 anaesthetists and 20 repeated measures).

Results

Cadavers were soft and flexible throughout all studies. Fig 1 shows the dissected left neck of a soft embalmed Thiel cadaver from an 87 year old female in the mortuary. Cadavers are kept within a secure bag and are not re-embalmed. All cadavers had full movement of limb joints and spine without impediment to use of ultrasound.

Tissue visibility

Visibility data followed a normal distribution. We made 168 measurements of visibility at 4 sites (interscalene, axillary, femoral, sciatic) on 3 structures (nerve, artery, muscle) by 2 raters on 7 occassions (2, 3, 5, 8, 11, 14, 28 weeks) after embalming. Visibility did not change between 2 to 28 weeks. Geometric mean nerve visibility was 5.4 (95%CI: 4.3 - 6.9) at 2 weeks and 4.9 (95%CI: 3.8 - 6.2) at 28 weeks, geometric mean ratio 1.1 (95%CI: 0.8 - 1.7) P=1.0. Geometric mean muscle visibility was 5.2 (95%CI: 4.2 - 6.5) at 2 weeks and 4.1 (95%CI: 3.3 - 5.0) at 28 weeks, geometric mean ratio 1.4 (95%CI: 0.9 - 1.9), P=1.0. Geometric mean artery visibility was 4.6 (95%CI: 3.7 - 5.7) at 2 weeks and 4.8 (95%CIP 3.8 - 5.9) at 28 weeks, geometric mean ratio 1.0(95%CI: 0.7 - 1.4), P=1.0.

Tissue displacement and brightness

Typical elastogram images from soft embalmed cadavers and patients are shown for interscalene block and femoral block (Fig 2). Tissue displacement in cadavers (Table 1) was similar for femoral and interscalene blocks [geometric mean ratio 1.02(95%CI: 0.59 - 1.78), P=0.86] and using 1ml and 5ml injection volumes [geometric mean ratio 0.84(95%CI: 0.70 - 1.01), P=0.19]. Displacement was similar between the first and eighth 1ml injection [geometric

mean ratio 0.56(95%CI: -0.30 - 1.43), P=0.67]. Using 5ml volumes, displacement was greater with the first compared to the eighth injection [geometric mean ratio 1.50(95%CI: 0.58 - 2.42), P<0.001].

Hydrolocation brightness in the cadaver was similar for femoral and interscalene blocks [geometric mean ratio 0.99(95%CI: 0.98 - 1.00), P=0.86] and 1ml and 5ml injection volumes [geometric mean ratio 0.84(95%CI: 0.83 - 0.85), P=0.19]. Mean (95%CI:) brightness was similar between the first and eighth 1ml injection [geometric mean ratio 1.01(95%CI: 0.96 - 1.06), P=1.0]. Using 5ml volumes, brightness was less with the first compared to the eighth injection [geometric mean ratio 0.94(95%CI: 0.89 - 1.00), P<0.001].

Stiffness

We visualised colour maps of Young's modulus at interscalene nerve root, median nerve and sciatic nerve sites in two soft embalmed Thiel human cadavers and in a patient and volunteer for comparison. One cadaver was 35 years old and embalmed for 267 days; the other was 75 years old and embalmed for 141 days. Shear wave colour maps in Fig 3 show similar anatomical distribution of Young's modulus for nerve sites in the cadaver compared to patients and volunteers (Fig 3). Measurements of cadaver SWE (Table 2) showed that intraneural Young's modulus was greater than extraneural Young's modulus [geometric mean ratio 3.05(95%CI: 2.98 - 3.12), P < 0.001], similar to humans[15]. Moreover cadaver, interscalene nerve root Young's modulus was less than median nerve Young's modulus [geometric mean ratio 0.60(95%CI: 0.58-0.62), p < 0.001]; and greater than sciatic nerve Young's modulus [geometric mean ratio 2.24(95%CI: 2.17- 2.31), P < 0.001]. Median nerve Young's modulus was greater than sciatic nerve Young's modulus [geometric mean ratio 3.71(95%CI: 3.59-3.84), P < 0.001]. The rank order of nerve stiffness was the same as in humans.

Durability

In a separate study 20 trainees conducted 934 left sided interscalene nerve blocks at the same site on the same cadaver over a 10-day period. Images of interscalene nerve roots and muscles are shown in Fig 4. All images show C5 and C6 nerve roots with the medial scalene muscle laterally and anterior scalene muscle medially. There was a small accumulation of fluid in the medial scalene muscle on days 7 and 10 compared to right interscalene control images., but the morphology of the nerve roots and anterior scalene and superficial tissues was preserved.

Discussion

We have demonstrated that the soft embalmed Thiel human cadaver has physical properties that enable functional task alignment during regional anaesthesia. Cadavers were similar in appearance to patients and joints were fully flexible. Tissue visibility, brightness, displacement strain secondary to perineural injection and stiffness were similar to that experienced when scanning and conducting UGRA on patients. With repeated injections, the cadaver remained intact and there was only small accumulation of perineural fluid in the scalenus medius muscle despite injecting blocks on 934 occasions over 10 days.

Using B-Mode ultrasound, characteristic anatomical features were discernible in the cadaver. For example, the reduced echogenicity of interscalene nerve roots in patients (Fig 2) secondary to the high ratio of fascicles to stromal tissue and the mixed echogenicity of the femoral (Fig 2) and median nerves (Fig 3) were similar in cadavers to that seen when imaging patients. Blood vessels were visible but not compressible.

However, an UGRA simulator should not only be able to demonstrate static anatomy but also to replicate the complex flow of local anaesthetic around nerves. We used strain elastography, regarded within cancer research[18] as a marker of palpation, one of the time-honoured methods of clinical examination. In the context of UGRA, elastography provided a dynamic image of strain, incorporating the relative displacement of both fluid and surrounding tissues, and enabled us to identify changes in the position, size and shape of tissue specific to each block. From our observations we may hypothesise that perineural strain patterns reflect bulk movement of fluid, displacement of soft tissue and reflection from fascial and tissue layers, and that this phenomenon is common to both patients[12] and soft embalmed Thiel cadavers during UGRA.

UGRA simulation training should also be safe, allow mistakes, and provide as many repeatable exercises as necessary in order to gain competence. In order to achieve this, simulator interaction should mimic clinical scenarios sufficiently in order to 'suspend belief'[19]. Our results showed that elastogram area did not change with sequential 1ml or 5ml injections, even when administered every 5 to 10 minutes. Our findings were corroborated by our recent intensive UGRA training workshops whereby individual trainees were invited to conduct left interscalene blocks on the same cadaver, at the same site repeatedly for 3 hours while being supervised one-to-one by an expert in regional anaesthesia. In all 934 blocks were performed using the same site in the same cadaver by 20 trainees over 10 days. The volume of injectate was between 500ml and 1,000ml. We noticed that with repeated injections per day, some Thiel moistening fluid accumulated within the medial scalene muscle, but with skin massage easily dispersed and drained, retaining the morphology of nerve roots and anterior scalene muscle. We do not know why fluid drains well in the soft embalmed cadaver. Possible reasons include spread of fluid

through tissue planes or osmotic differences between Thiel moistening fluid and embalming fluid within the Thiel tanks.

The drainage properties of the soft embalmed Thiel human cadaver simulator provide a realistic and highly durable simulator, providing good conditions for intensive, repeated injections during UGRA training courses, and offers the opportunity to objectively measure learning curves in an environment that provides good repeatability conditions.

We may also attribute the durability of our cadavers to their elastic properties. Our measurements of interscalene and sciatic stiffness in the soft embalmed cadaver reflected available human data, both with regard to absolute measurements and confirmed the 2 to 3 fold difference between neural and perineural Young's modulus that we had previously noted[15]. A recent study investigating the stiffness of head and neck glandular tissue and muscle showed that Young's modulus was approximately 20% higher in Thiel embalmed cadavers compared to historical data on volunteers[20]. High stiffness of the median nerve in the soft embalmed cadaver (consistent with recent work by Kantarci and colleagues[21]) and low stiffness in the sciatic nerve reflects the site-specific values measured in our volunteers. Arm position and age may account for high median nerve stiffness. For example, Gennisson et al[22] showed that biceps muscle stiffness varied between 5.4kPa when the elbow was bent to 90^0 and 29.5kPa when extended to $165^{0.}$. High median nerve stiffness in the cadaver was similar to results from a study in volunteers, particularly when matched for age[16], and probably reflects the deterioration of muscle morphology and increased muscle stiffness in the sixth to seventh decade.

Cadaver availability was limited when we conducted this study. Our experience is that cadavers are not identical and vary in response to embalming and storage. We anticipate that because different interventions have different needs, cadaver selection is important in order to provide the most valid cadaver model.

In light of both ours and surgeons' experience using cadavers up to a maximum of 3 years old for training courses[20], the University of Dundee has built a new state of the art Thiel facility costing £2.5 million, 40% of which was paid for by local fundraising, http://www.millionforamorgue.com/new-forensic-centre-of-excellence. The facility now handles 80 Thiel embalmed cadavers per year for medical and dental teaching. On-going studies are investigating the optimal mix of embalming solution for specific surgical procedures.

However, we are also aware of our study limitations. We did not wish to compare area and shear speed measurements in the cadaver with matched humans because we wished to show that the soft embalmed Thiel cadaver is a simulator that has the potential to suspend belief. Validating the cadaver with humans would not have been possible as the emblaming process does not exactly replicate tissue morphology. Thus our study focused on physical characteristics and functional alignment but not the effectiveness of simulation, the degree to which skills acquired on the cadaver are translatable to the real world[23]. Effective translation may be judged by a trainees ability to suspend belief during simulated tasks, solve complex, unstructured problems, and prioritize, communicate and enact critical decisions[24].

Our feeling is that theoretical knowledge reinforced by repeated practice on the Thiel simulator has the potential to translate both high-level knowledge and competency to clinical practice.

Our next step is to translate our simulator into the process of simulation by using it as an educational tool for the teaching of UGRA in trainee anaesthetists[25]. Educational validation will require us to define the educational process, learning outcomes and assessment of competency[26]. Unlike the traditional clinical apprentice model, a stable, high fidelity

simulator should offer the opportunity to provide measurable, consistent training by standardizing both teaching, assessment and learning[27].

Irrespective of educational discussion our approach to assessment of our soft embalmed Thiel simulator within our study was focused, not simply on the appearance of the soft embalmed Thiel cadaver, but on its function within a specific context, i.e. regional anaesthesia. We agree with educationalists[6] that merely providing a high fidelity simulator does not equate with better training effectiveness, and that we need to test the dynamics of this simulator within a variety of simulation-based scenarios allied to educational need. Ultimately any simulator should be judged on its capacity to enhance personal learning irrespective of its appearance. Nevertheless we anticipate that both the appearance and dynamic response of our simulator can suspend belief sufficiently to enhance the quality of regional anaesthesia training.

In conclusion, we have demonstrated using objective ultrasound measurements of tissue brightness, strain and stiffness that the soft embalmed Thiel cadaver is a faithful representation of patient soft tissue characteristics during UGRA, that it provides excellent, repeatable conditions for the simulation of UGRA, and that it now offers the opportunity to objectively measure UGRA learning curves in a stable environment.

Acknowledgements

We wish to thank Supersonic Imagine for use of an Aixplorer shear wave ultrasound machine

Contributions

Dr Shilpa Munirama had the original idea, designed and conducted the studies and wrote the paper

Dr Roos Eisma provided anatomy support

Malachy Columb provided statistical support

Prof George A Corner provided technical ultrasound support

Dr Graeme A McLeod had the original idea, designed and conducted the studies and wrote the paper

References

1 Flin R, Patey R, Glavin R, Maran N. Anaesthetists' non-technical skills. *British journal of anaesthesia* 2010; **105**: 38-44

2 Adhikary SD, Hadzic A, McQuillan PM. Simulator for teaching hand-eye coordination during ultrasound-guided regional anaesthesia. *British journal of anaesthesia* 2013; **111**: 844-5

3 Hocking G, Hebard S, Mitchell CH. A review of the benefits and pitfalls of phantoms in ultrasound-guided regional anesthesia. *Regional anesthesia and pain medine* 2011; **36**: 162-70

4 Grottke O, Ntouba A, Ullrich S, et al. Virtual reality-based simulator for training in regional anaesthesia. *British journal of anaesthesia* 2009; **103**: 594-600

5 Cheung JJ, Chen EW, Al-Allaq Y, et al. Acquisition of technical skills in ultrasound-guided regional anesthesia using a high-fidelity simulator. *Studies in health technology and informatics* 2011; **163**: 119-24

6 Hamstra SJ, Brydges R, Hatala R, Zendejas B, Cook DA. Reconsidering fidelity in simulation-based training. *Academic medicine : journal of the Association of American Medical Colleges* 2014; **89**: 387-92

7 Thiel W. [The preservation of the whole corpse with natural color]. *Annals of anatomy = Anatomischer Anzeiger : official organ of the Anatomische Gesellschaft* 1992; **174**: 185-95

8 Benkhadra M, Faust A, Ladoire S, et al. Comparison of fresh and Thiel's embalmed cadavers according to the suitability for ultrasound-guided regional anesthesia of the cervical region. *Surgical and radiologic anatomy : SRA* 2009; **31**: 531-5

9 Eisma R, Wilkinson T. From "silent teachers" to models. *PLoS biology* 2014; **12**: e1001971

10 McLeod G, Eisma R, Schwab A, Corner G, Soames R, Cochran S. An evaluation of Thiel-embalmed cadavers for ultrasound-based regional anaesthesia training and research. . *Ultrasound* 2010; **18**: 125-9

11 Munirama S, McLeod G, Eisma R, et al. Application of sonoelastography to regional anaesthesia: a descriptive study with the Thiel embalmed cadaver model. . *Ultrasound* 2012: 41-8

12 Munirama S, Satapathy AR, Schwab A, et al. Translation of sonoelastography from Thiel cadaver to patients for peripheral nerve blocks. *Anaesthesia* 2012; **67**: 721-8

13 Lacourpaille L, Hug F, Bouillard K, Hogrel JY, Nordez A. Supersonic shear imaging provides a reliable measurement of resting muscle shear elastic modulus. *Physiological measurement* 2012; **33**: N19-28

14 Wells PN, Liang HD. Medical ultrasound: imaging of soft tissue strain and elastiCI:ty. *Journal of the Royal Society, Interface / the Royal SoCI:ety* 2011; **8**: 1521-49

15 Munirama S, Joy J, Eisma R, Corner G, Cochran S, McLeod G. Images in anesthesiology: shear wave elastography: novel technology for ultrasound-guided regional anesthesia. *Anesthesiology* 2013; **119**: 698

16 Eby SF, Cloud BA, Brandenburg JE, et al. Shear wave elastography of passive skeletal muscle stiffness: Influences of sex and age throughout adulthood. *Clinical biomechanics* 2015; **30**: 22-7

17 Moayeri N, Groen GJ. Differences in quantitative architecture of sciatic nerve may explain differences in potential vulnerability to nerve injury, onset time, and minimum effective anesthetic volume. *Anesthesiology* 2009; **111**: 1128-34

18 Evans A, Whelehan P, Thomson K, et al. Differentiating benign from malignant solid breast masses: value of shear wave elastography according to lesion stiffness combined with greyscale ultrasound according to BI-RADS classification. *British journal of cancer* 2012; **107**: 224-9

19 Allen J, Hays RT, Buffardi LC. Maintenance Training Simulator Fidelity and Individual Differences in Transfer of Training. *Human Factors: The Journal of the Human Factors and Ergonomics SoCI:ety* 1986; **28**: 497-509
20 Joy J, McLeod G, Lee N, et al. Quantitative assessment of Thiel soft-embalmed human cadavers using shear wave elastography. *Annals of anatomy = Anatomischer Anzeiger : official organ of the Anatomische Gesellschaft* 2015; **202**: 52-6
21 KantarCI: F, Ustabasioglu FE, Delil S, et al. Median nerve stiffness measurement by shear wave elastography: a potential sonographic method in the diagnosis of carpal tunnel syndrome. *European radiology* 2014; **24**: 434-40
22 Gennisson JL, Deffieux T, Mace E, Montaldo G, Fink M, Tanter M. Viscoelastic and anisotropic mechanical properties of in vivo muscle tissue assessed by supersonic shear imaging. *Ultrasound in medicine & biology* 2010; **36**: 789-801
23 Maran NJ, Glavin RJ. Low- to high-fidelity simulation - a continuum of medical education? *Medical education* 2003; **37 Suppl 1**: 22-8
24 Murray DJ. Progress in simulation education: developing an anesthesia curriculum. *Current opinion in anaesthesiology* 2014; **27**: 610-5
25 Meyer GF, Wong LT, Timson E, Perfect P, White MD. Objective fidelity evaluation in multisensory virtual environments: auditory cue fidelity in flight simulation. *PloS one* 2012; **7**: e44381
26 Neal JM. Education in regional anesthesia: caseloads, simulation, journals, and politics: 2011 Carl Koller Lecture. *Regional anesthesia and pain medicine* 2012; **37**: 647-51
27 Laurent DA, Niazi AU, Cunningham MS, et al. A valid and reliable assessment tool for remote simulation-based ultrasound-guided regional anesthesia. *Regional anesthesia and pain medicine* 2014; **39**: 496-501

Table legend

Table 1. Geometric mean B-Mode ultrasound displacement (cm^2) and brightness (0-255 scale) with regard to site, volume, injection sequence and the interaction of site:volume and sequence:volume. Mean (95%CI:) displacement and brightness in cadavers was similar for femoral and interscalene blocks, 1ml and 5ml injection volumes. There was no sequential accumulation of fluid.

Table 2. Geometric mean Young's modulus (kPa) with regard to intraneural:extraneural pairs, anatomical site and their interaction. Intraneural Young's modulus was greater than perineural Young's modulus, $p<0.001$. The rank order (highest to lowest) of Young's modulus was median nerve > interscalene nerve root > sciatic nerve. Differences existed between all neural:site comparisons other than between median:extraneural and sciatic:intraneural combinations, $P = 0.67$.

Figures

Fig 1. Example of neck dissection in soft embalmed Thiel cadaver. Brachial plexus roots seen between the anterior and middle scalene muscles. The abbreviations are: VN, vagus nerve; CCA, common carotid artery; AS, anterior scalene; MS, middle scalene; PN, phrenic nerve crossing anterior scalene muscle; O, omohyoid muscle; C5, C6, C7- anterior rami.

Fig 2. Strain and brightness characteristics in soft embalmed Thiel cadaver and patients during interscalene and femoral nerve block. Column A: interscalene block in the soft embalmed Thiel cadaver; column B: interscalene block in patient; column C: femoral block conducted in the soft embalmed Thiel cadaver; column D: femoral block conducted in patient. Upper images are the standard B-Mode image with abbreviations: AS, anterior scalene; MS, middle scalene; FA, femoral artery; FN, femoral nerve. Middle images highlight the femoral nerve in blue and the spread of fluid in yellow. Lower coloured elastograms show tissue displacement associated with a 5ml bolus of injectate in both soft embalmed Thiel cadaver and patients. Increased strain is associated with progression from yellow to orange to red. Fluid spread is smaller than strain because tissues are displaced secondary to fluid injection.

Fig 3. B-Mode and SWE ultrasound images of interscalene nerve roots and median nerves in Thiel embalmed soft cadaver and human. Column A: interscalene nerve roots in the soft embalmed Thiel cadaver; column B: interscalene nerve roots in patient; column C: median nerve in the soft embalmed Thiel cadaver; column D: median nerve in volunteer; column E: sciatic nerve in the soft embalmed Thiel cadaver; column F: sciatic nerve in volunteer. Upper images are SWE and lower images are standard B-Mode ultrasound. Within the SWE images the coloured area gives a pictorial representation of Young's modulus. For both interscalene nerve roots and sciatic nerves Young's modulus gradient is represented by: dark blue, 0 - 7kPa; light blue, 7 - 14kPa; green, 14 -21kPa; yellow/orange 21 – 28kPa; red, 28 – 35kPa. For median nerve Young's modulus gradient is represented as: dark blue, 0 - 18kPa; light blue, 18 - 36kPa; green, 36 - 54kPa; yellow/orange 54 – 72kPa; red, 72 – 90kPa. Regions of interest (ROI) used to measure Young's modulus not shown. Coloured areas correspond to stiff interscalene nerve roots, median nerve, sciatic nerve and stiff connective tissue in both

the soft embalmed Thiel cadaver and humans. Colour maps indicate stiffness of tissues within similar ranges in Thiel cadaver and humans. Note that order of stiffness in Thiel cadaver is the same as in human: median > interscalene > sciatic

Fig 4. B-Mode images from a study investigating learning curves of anaesthetic trainees. Twenty trainees performed left sided interscalene block at the same site, in the same cadaver over 10 days. Column A represents images taken on day 7 and column B represents images taken on day 10. The upper images are right side control images of the interscalene region. The middle images show left side interscalene region recorded at 0900h on days 7 and 10. The lower images show the left side interscalene image at 1500h on day 7 and day 10 after 120 needle insertions and injection of at least 60ml Thiel embalming fluid each day. White arrow indicates path of block needle. Images show small accumulation of fluid in medial scalene muscle compared to right sided control, but retention of nerve root, anterior scalene and superficial tissue morphology. Between day 7 and day 10, at least 150ml of fluid was injected but minimal change present in middle scalene muscle.

Fixed term	Area (cm^2) mean (95%CI)	Brightness (0 – 255) mean (95%CI)
Site		
Interscalene	2.34(1.96 - 2.79)	133.2 (132.0 - 133.2)
Femoral	2.39 (1.99 - 2.87)	132.1 (130.9 - 133.2)
Volume		
1ml	2.17 (1.80 - 2.62)	121.6 (120.5 - 122.7)
5ml	2.58 (2.17 - 3.07)	144.7 (143.4 - 145.9)
Injection sequence		
First	4.58 (3.34 – 6.29)	138.7 (136.6 - 140.9)
Second	4.58 (3.34 – 6.29)	124.2 (121.4 – 127.1)
Third	4.58 (3.34 – 6.29)	137.4 (134.7 - 140.1)
Fourth	4.58 (3.34 – 6.29)	133.2 (131.1 - 135.3)
Fifth	4.58 (3.34 – 6.29)	141.9 (139.4 - 144.4)
Sixth	4.58 (3.34 – 6.29)	120.1 (118.4 - 121.9)
Seventh	4.58 (3.34 – 6.29)	124.9 (123.0 - 126.8)
Eighth	1.63 (1.11 – 2.39)	142.5 (139.8 - 145.2)
Site*volume		
Interscalene: 1ml	2.03 (1.55 - 2.67)	127.3 (125.6 - 129.1)
Interscalene: 5ml	2.69 (2.16 - 3.36)	139.3 (137.8 - 140.8)
Femoral: 1ml	2.32 (1.79 - 3.01)	116.1 (114.6 - 117.5)
Femoral: 5ml	2.47 (1.88 - 3.24)	150.3 (148.3 - 152.3)
Sequence*volume		
1^{st} injection: 1ml	3.97 (2.44 - 6.46)	128.4 (125.4 - 131.5)
8^{th} injection: 1ml	2.26 (1.55 – 3.30)	127.5 (125.2 - 129.9)
1^{st} injection: 5ml	5.28 (3.57 - 7.81)	149.8 (147.0 - 152.7)
8^{t} injection: 5ml	1.17 (1.16 – 2.68)	159.2 (153.7 - 164.8)

Fixed term	Estimated [adjusted] Mean (95%CI) shear wave speed (kPa)
Neural	
Extraneural	10.5 (6.5 - 17.0)
Intraneural	32.2 (20.0 - 52.1)
Site	
Interscalene	18.5 (9.7 - 35.3)
Median	31.9 (18.4 - 55.3)
Sciatic	10.6 (5.6 - 20.1)
Neural*Site	
Extraneural: Interscalene	12.7 (6.3 - 25.7)
Extraneural: Median	18.8 (9.7 - 36.3)
Extraneural: Sciatic	4.8 (2.4 - 9.8)
Intraneural: Interscalene	26.9 (12.7 - 57.2)
Intraneural: Median	54.0 (27.7 - 105.3)
Intraneural: Sciatic	23.0 (10.9 - 48.9)

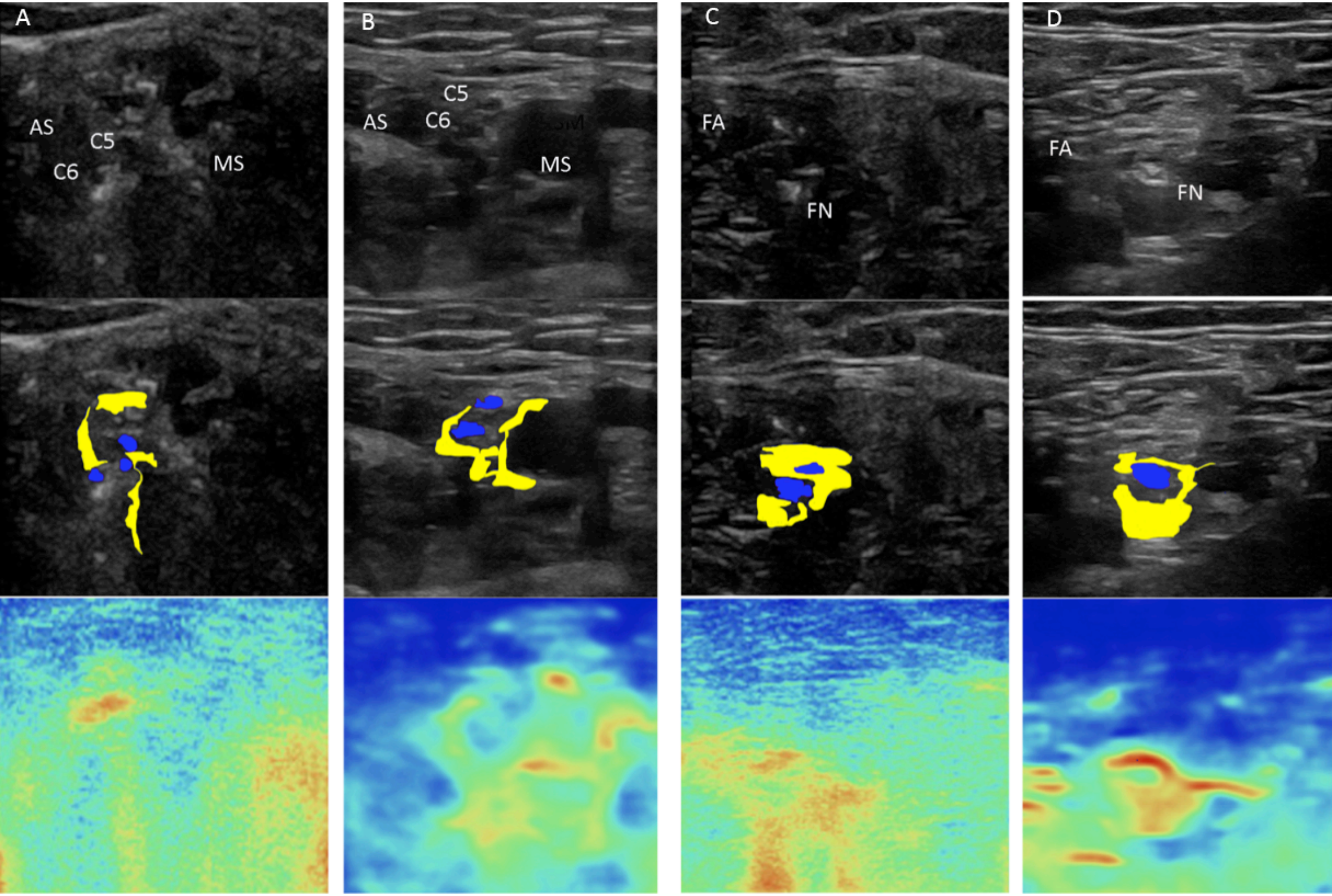
A
AS
C5
C6
MS
B
C5
AS
C6
MS
C
FA
FN
D
FA
FN

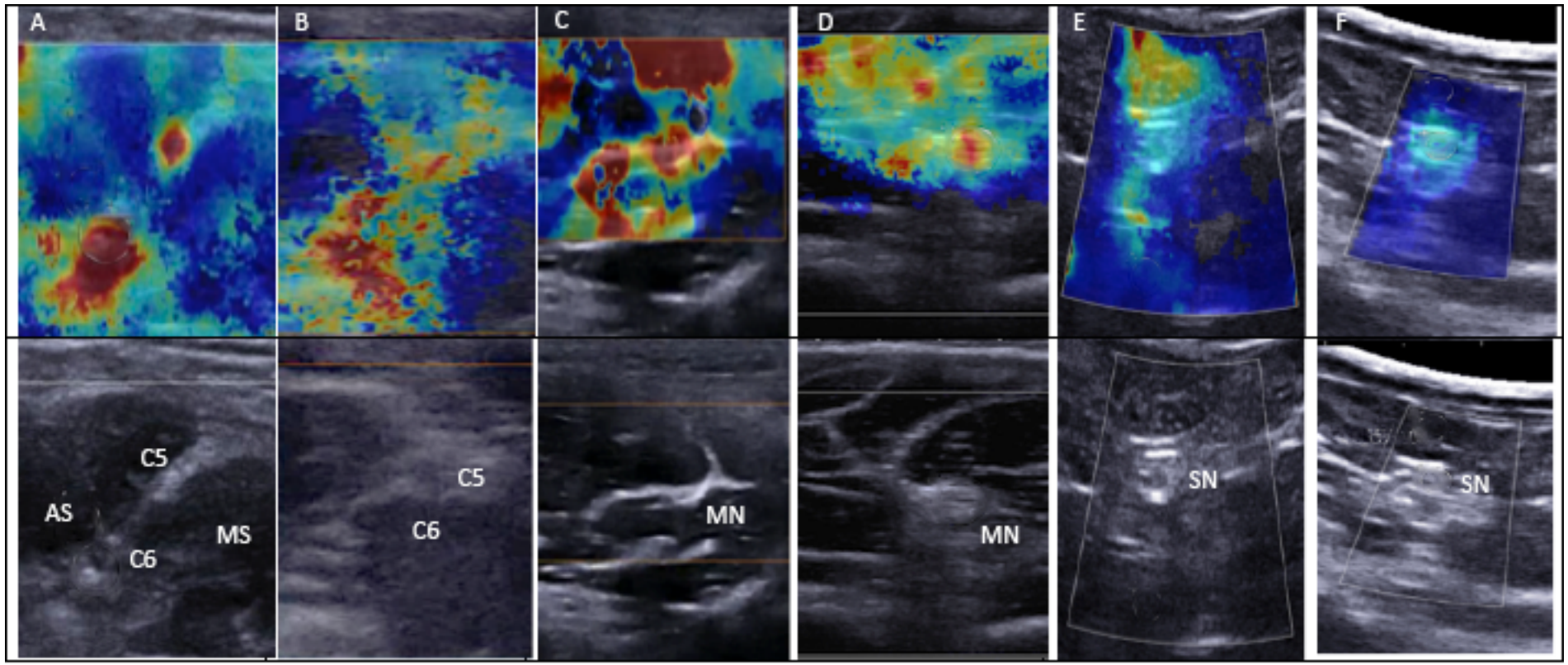
A
B
C
D
E
F
C5
AS
MS
C6
C5
C6
MN
MN
SN
SN

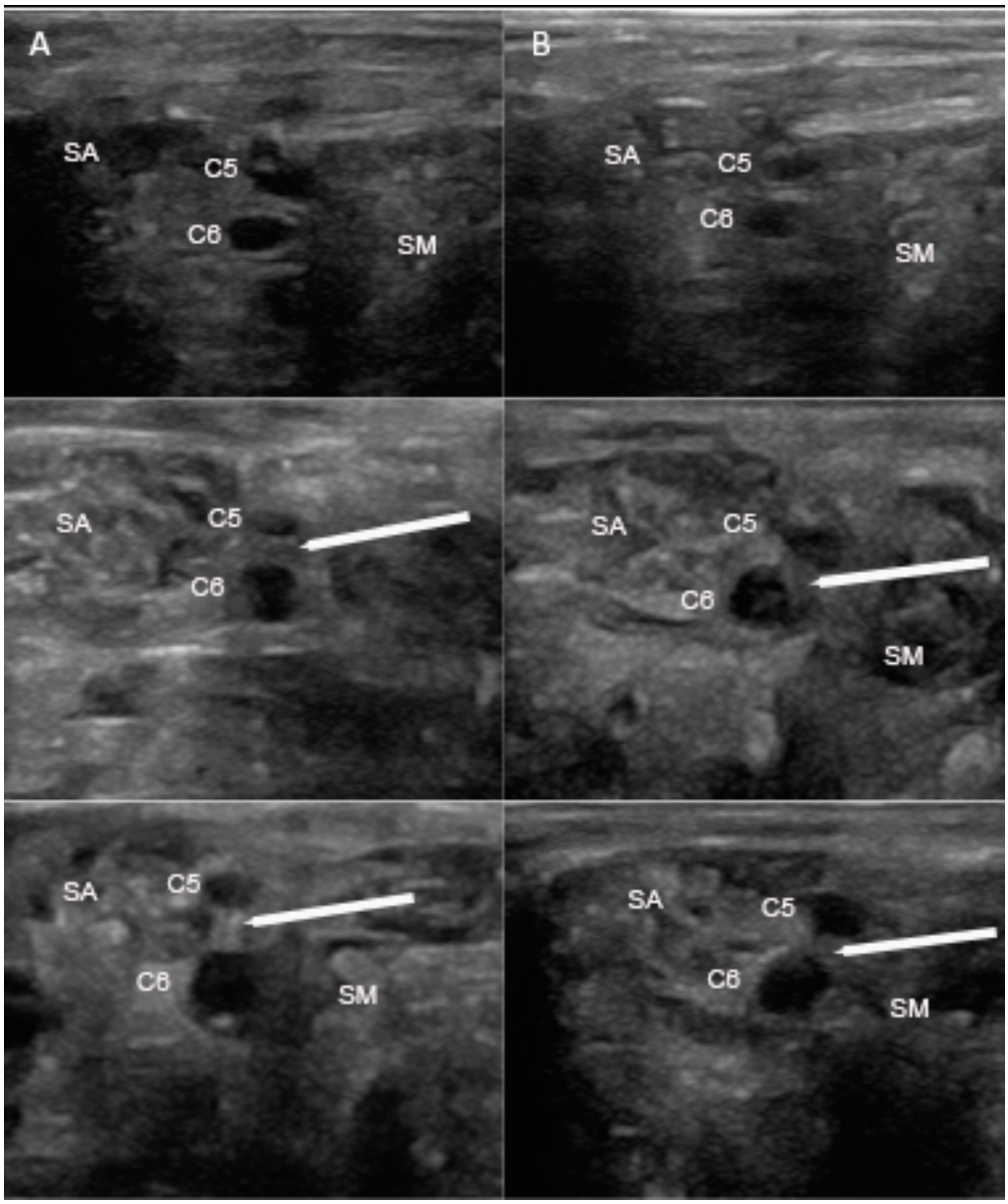
A
SA
C5
C6
SM
B
SA
C5
C6
SM
SA
C5
C6
SA
C5
C6
SM
SA
C5
C6
SM
SA
C5
C6
SM